https://doi.org/10.5194/nhess-2022-177
Preprint. Discussion started: 19 July 2022
© Author(s) 2022. CC BY 4.0 License.

Natural Hazards and Earth System Sciences
Discussions

Development and validation using ground truth of a method to identify potential release areas of snow avalanches based on watershed delineation

Cécile Duvillier[1], Nicolas Eckert[1], Guillaume Evin[1], Michael Deschâtres[1]

[1]Univ. Grenoble Alpes, INRAE, UR ETNA, Grenoble, France
Correspondence to: Nicolas Eckert (nicolas.eckert@inrae.fr)

Keywords: Snow Avalanches, Potential Release Area, Validation, Confusion Matrix, Watershed, French Alps.

Abstract. Snow avalanches are a prevalent threat in mountain territories. Large-scale mapping of avalanche prone terrain is a prerequisite for land-use planning where historical information about past events is lacunar. To this aim, the most common approach is the identification of Potential Release Areas (PRAs) followed by numerical avalanche simulations. Existing methods for identifying PRAs rely on terrain analysis. Despite their efficiency, they suffer from i) a lack of systematic validation on the basis of adapted metrics and past observations over large areas and ii) a limited ability to distinguish PRAs corresponding to individual avalanche paths. The latter may preclude performing numerical simulations corresponding to individual avalanche events, questioning the realism of resulting hazard assessments. In this paper, a method that well identifies individual snow avalanche PRAs based on terrain parameters and watershed delineation is developed, and confusion matrices and accuracy scores computed both in terms of PRA numbers and areas are proposed to test and evaluate it. Confrontation to an extensive cadastre of past avalanche limits from different massifs of the French Alps used as ground truth leads to high accuracy rates, between 89.8% and 93.5% in numbers and 96.2% and 97.1% in areas. This shows the applicability of the method to the French Alps context. A sensitivity study is performed, highlighting the most important steps to reach high accuracy in PRA detection, among which the strong role of watershed delineation to identify the right number of individual PRAs. Outlooks for further progresses are discussed. Notably, the proposed data and evaluation framework could be used for additional developments of the method, and to benchmark existing and/or new PRA detection methods.

1. Introduction

In mountain territories, snow avalanches are a prevalent threat, resulting in casualties and damages to buildings and critical infrastructures (Amman and Bebi, 2000; Braun et al., 2020). No countermeasures can be taken after the avalanche initiation because the time before the damageable impact is generally less than one minute. Identification of avalanche-prone terrain and subsequent hazard/risk mapping, supplemented, if necessary, by defence structures, is, therefore, the most efficient way to reduce death tolls and costs on the long range for settlements downslope (Arnalds et al., 2004; IRASMOS consortium, 2009; Eckert et al., 2012). To this aim, availability of historical information concerning avalanche location, frequency and magnitude is crucial (Giacona et al., 2017). For instance, spatial statistics can be used to interpolate the data available from a sample of paths (Lavigne et al. 2012; 2017) in order to assess avalanche hazard over large areas. However, even in the best-

https://doi.org/10.5194/nhess-2022-177
Preprint. Discussion started: 19 July 2022
© Author(s) 2022. CC BY 4.0 License.

Natural Hazards and Earth System Sciences
Discussions

documented areas, historical information is far from exhaustive, and, in many mountain territories, it remains quasi-absent. The standard approach to delineate avalanche-prone terrain is then the automatic identification of Potential Release Areas (PRAs) on the basis of terrain analysis followed by numerical (Naaim et al., 2004; Bartelt et al., 2012) and/or statistical-numerical avalanche simulations (Keylock et al., 1999; Eckert et al., 2010; Fischer et al., 2015). In these, PRA identification supplemented by snow cover information from neighbouring meteorological stations or reanalyses provide the input conditions for avalanche simulations, which define hazard and risk levels downslope (Gruber and Bartelt, 2007; Barbolini et al., 2011; Bühler et al., 2018; Ortner et al., 2022). Wider benefits can also arise for the systematic detection of PRAs: better understanding of the avalanching process at large scale, identification of areas that need to be reforested to reduce hazard and risk, etc.

Snow avalanche PRA detection methods from terrain analysis belong to the class of susceptibility mapping methods, which are widely used for many mountain hazards (Bertrand et al., 2013; Eckert et al., 2018). Several automatic snow avalanche PRA detection methods are now available in the literature, and, since first proposals (Maggioni et al., 2002; Maggioni and Gruber, 2003), different extensions have been implemented (e.g., Sykes et al., 2021). For example, while PRAs were historically assessed independently from snow and weather conditions, Chueca Cía et al. (2014) developed a multi-criteria analysis for snow avalanche susceptibility mapping that uses wind directions and snowdrift to identify PRAs in a dynamic way. Also, while most of existing approaches are deterministic (e.g., Bühler et al., 2013), Veitinger et al. (2016) apply fuzzy logic to relate past release areas to slope, roughness and a shelter wind index. Similarly, Kumar et al. (2019) detect PRAs in the Lahaul region of Western Himalaya using a probabilistic occurrence ratio and Yariyan et al. (2020) identify more broadly "avalanche sensitive areas" using different statistical models.

Most of PRA detection methods use forest cover and geomorphologic features such as slope, plan curvature, aspect, and distance to ridges as decisive factors. For instance, distance to ridges is generally retained as a useful quantity because it is a proxy for snowdrift, which is known to be an important triggering factor (e.g., Lehning et al., 2000). Also, forests limit avalanches release by anchoring snowpack and, more generally, lower avalanche hazard and risk downslope (Bebi et al., 2009; Zgheib et al., 2022), so that presence of a dense forest is often considered as sufficient to exclude a given location from PRAs (e.g. Maggioni et al. 2002). However, there are many disagreements between researchers about i) the exact choice and respective importance of the different factors to be used in PRA detection, and ii) the best parameter values/thresholds to be specified to reach maximal accuracy. For instance, in Maggioni et al. (2002), retained factors are slope, aspect, curvature, forest presence, and distance to ridges, whereas Bühler et al. (2013) consider, in addition, information about roughness and flow direction. Also, it is generally admitted that, for slopes steeper than 60°, snow accumulation is low (e.g., Maggioni and Gruber, 2003). Yet, the range of slopes to be retained in automated PRA detection remains debated, as i) the true range of slopes over which avalanche release is actually possible remains uncertain (e.g., it varies with snow conditions, Schweizer et al., 2003; Naaim et al., 2013), ii) it is not independent of the chosen Digital Elevation Model (DEM) resolution. Hence, the 28-60° range is selected in Veitinger et al. (2016) using a DEM with a 2m resolution, but 28-55° is preferred in Aydin and Eker (2017) using a DEM with a resolution of 10 m, and 25-40° is used in Kumar and al., (2019). Similarly, the range of elevations where PRAs are searched is very dependent on the region of the world. Aydin and Eker (2017) consider the 1000-4000m a.s.l. range in Turkey, while Kumar et al. (2019) adapt this range to higher mountain environments with a minimal elevation fixed to 2800m a.s.l.

Eventually, dynamic PRA mapping methods consider snow and weather factors. Chueca Cía et al. (2014) make

https://doi.org/10.5194/nhess-2022-177
Preprint. Discussion started: 19 July 2022
© Author(s) 2022. CC BY 4.0 License.

use of a multi-scale roughness adjusted to snow depth and of a shelter wind index whereas other parameters describing the climatology (snowfall, temperature change, precipitation), lithology and land use are accounted for in Yariyan et al. (2020).

Important characteristics of existing PRA detection methods is their limited ability to distinguish PRAs corresponding to individual avalanche paths/events. Indeed, PRA detection methods mostly focus on terrain characteristics at the pixel scale. Hence, they do not easily segment large areas where factors are favourable to avalanche release (suitable slope, roughness, etc.) in different PRAs compatible with the physical processes involved in snow avalanching (Schweizer, 2003). This may lead to unrealistically wide PRAs that, on the field, correspond to different avalanche paths/events. This drawback is critical for their use for hazard assessment downslope, as it may preclude performing numerical simulations corresponding to realistic individual avalanche events.

To evaluate the performance of PRA detection methods, most studies use recorded avalanches (Maggioni and Gruber, 2003; Bühler et al., 2013; Veitinger et al., 2016), with historical information provided either by local observers after each event or by interviewing local people. Evaluation is often qualitative, and confront the detected PRAs with avalanches boundaries obtained from residents (Aydin and Eker, 2017), from aerial or satellite photographs (Bühler et al., 2019) or from avalanche simulations (Nolting et al., 2018). Over the recent years, more quantitative evaluation methods have gained popularity in the snow avalanche field, notably to assess the efficiency of snow avalanche detection from satellite images (e.g., Karas et al., 2021), or of the prediction of snow avalanche occurrences on the basis of snow and weather conditions (Sielenou et al., 2021). These advanced evaluation approaches use different metrics to quantify overall performance based on long historical records or large-scale field data taken as ground truth. Considered metrics include probabilistic occurrence ratios (summed-up as confusion matrices) and receiver operating characteristic – area under curve (ROC-AUC criteria). To our knowledge, despite the strong development over the last years of competing PRA detection methods, these quantitative evaluation methods remain very seldom used so far (Bühler et al., 2018) to evaluate their respective efficiency, advantages and limits in an objective way. This lack is partially attributable to the fact that information about avalanche release areas is even sparser than information about avalanches in general, as avalanche release typically occurs in remote uninhabited and/or difficult/dangerous-to-access areas.

On this basis, we propose in this paper an automatic detection method that well identifies individual PRAs, and a framework to test and evaluate it. The objective of our approach is to identify all locations where an avalanche can potentially occur. There is no notion of frequency, meaning that avalanche releases may occur very frequently in certain PRAs we detect, and extremely rarely in others. Also, our definition of an individual PRA is the maximal extension corresponding to the release of a single avalanche event. Hence, in practice, many avalanche releases may concern a (potentially small) fraction of a single PRA, especially for the largest PRAs we detect. Following existing literature, our method uses topographical parameters (minimal elevation, range of slopes, maximum distance to ridges) and presence of forests as key factors. Main novelty is to include watershed delineation within the PRA identification, which provides spatial entities more comparable to avalanche paths. Development of the proposed method is guided by an extensive cadastre of past avalanche limits from different massifs of the French Alps used as ground truth. Several quantitative criteria are used to assess the performance of the method, but also to perform a sensitivity analysis highlighting the most important steps to reach high accuracy in PRA detection. Obtained accuracy rates in different massifs show the efficiency of the proposed method in the overall French Alps

https://doi.org/10.5194/nhess-2022-177
Preprint. Discussion started: 19 July 2022
© Author(s) 2022. CC BY 4.0 License.

context. We also demonstrate the strong role of watershed delineation to identify the right number of individual PRAs. In what follows, Sect. 2. presents the different datasets used. Sect. 3 introduces the proposed PRA detection method and evaluation framework. Sect. 4 details the results for considered test areas. Sect 5. sums up the main outcomes of the work, discusses pro's and con's of the proposed approach, and points out outlooks for further applications and developments.

2 Data

2.1 Study areas

In this paper, we focus on the French Alps and its classical segmentation into 23 massifs for snow-climate reanalyses and operational snow avalanche forecasting (e.g., Durand et al.; 2009a; 2009b; Evin et al., 2021). Despite the high exposure to snow avalanche risk of this territory, no automated PRA detection method was systematically applied in it so far. For this study, three entire massifs with different characteristics are specifically considered to illustrate and evaluate the detection method: Mont-Blanc, Chartreuse, and Maurienne (Figure 1). In addition, a focus is made on a smaller test area close to the town of Chamonix, so as to highlight some results and deepen the analyses at a fine spatial resolution.

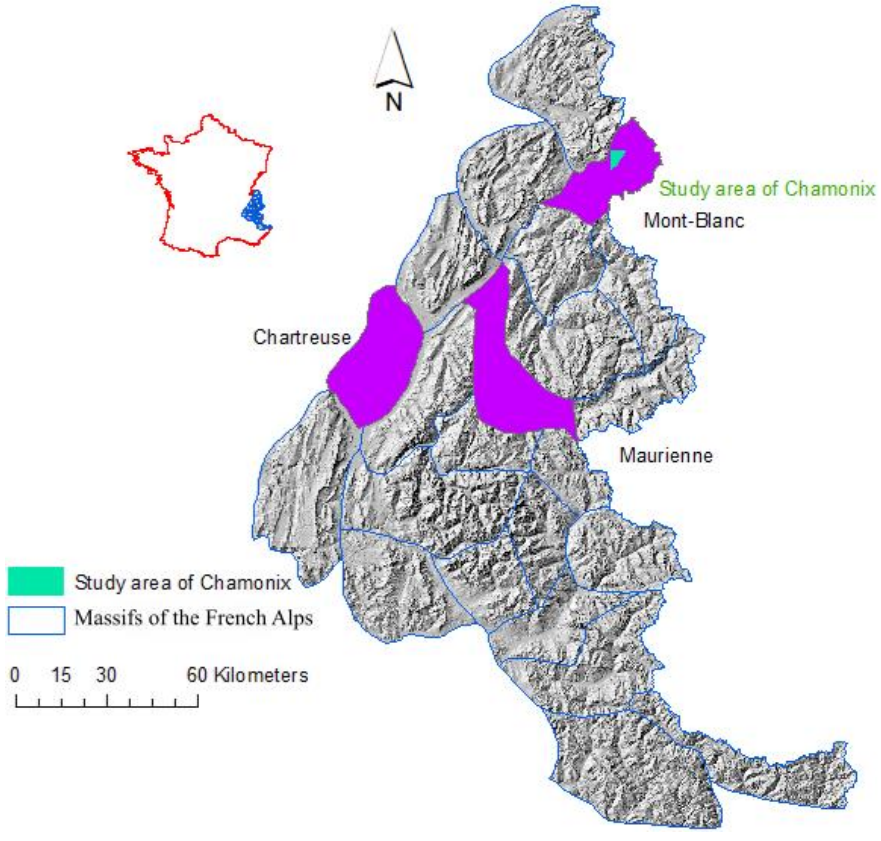

Figure 1 : Study areas: 3 entire massifs (within the 23 massifs of the French Alps) and a highlighted test area close to the town of Chamonix Mont-Blanc and included within the Mont-Blanc massif. Digital Elevation Model ©IGN.

https://doi.org/10.5194/nhess-2022-177
Preprint. Discussion started: 19 July 2022
© Author(s) 2022. CC BY 4.0 License.

The Mont-Blanc massif reaches an elevation of 4,809 m a.s.l. at the Mont-Blanc summit (top of Western Europe), and it is mainly composed of granite and gneiss. The valley of Chamonix is reputed for mountaineering, but also to be extremely exposed to snow avalanches. A tragic example is the snow avalanches of Montroc (9 February 1999), which led to the loss of twelve residents and the devastation of fourteen chalets (Ancey et al., 2000). The massif of Chartreuse is a massif of the Prealps, mainly composed of limestone. This massif is less subject to snow avalanches because of its lower elevation (highest point is Chamechaude at 2,082 m a.s.l.), but destructive snow avalanches occurred in it in the past, such as in Saint-Hilaire-du-Touvet (Ancey et al., 1999). The Maurienne massif has an intermediate elevation (highest peak reaches 3,160 m a.s.l.). Its economy is strongly oriented towards winter sports, and several of its large ski areas are threatened by avalanches.

2.2 DEM and forest cover

Topographic information used in the proposed PRA detection method is classically derived from a DEM. We used the reference 25 m resolution DEM from the French National Geographical Institute (IGN). While DEM with finer resolutions are now easily available, sensitivity tests (not shown) indicated that these did not improve accuracy scores (Sect. 3.4) significantly, whereas the computational burden became much higher. We therefore chose to stick on this 25 resolution, as a good compromise to i) detect the right number and areas of PRAs (even if being certainly less precise in terms of PRA boundaries that finer resolutions, e.g. Bühler et al., 2013), and ii) being ultimately applicable over very large areas at reasonable computational costs.

In addition to the DEM, our method considers forest cover as input data. For the French Alps, three nation-wide forest cover databases can potentially be used:

- The forest database (DB forest) provided by IGN obtained from the photo-interpretation of aerial infrared photographs. 32 classes of vegetation are available (notably, as function of tree species: Aleppo pine, coniferous trees, scotch pine, etc., ADEME and IGN, 2019). This data was created in 2013;
- Corine land cover is a database of land cover based on satellite imagery, which considers five classes of vegetation (artificial surfaces, agricultural areas, forests and semi natural areas, wetlands, and water bodies, Caetano et al., 2009). It is updated every 6 years, and the 2012 version was considered for the sake of comparison with the IGN data;
- Theia database is provided by the Center Expertise Scientifique (CES), which extracts data about land use, soil humidity and snow cover from Sentinel 2A and 2B satellites (Baghdadi et al., 2021). The 2016 version was selected as the closest from 2013.

Our PRA detection method uses forest presence/absence only. We thus derived this information for the three databases in our test areas. Despite the overall quality of the three nation-wide forest cover database, visual comparison to the aerial photograph of 2012 (ground truth, Figure 2) shows that the forest presence information from Corine land cover is sometimes not accurate enough in areas where forest is not well separated from grasslands and fields. In this example, Theia appears as better in terms of forest boundaries, but is less accurate than the IGN DB forests (some forested areas are missing in Theia, whereas they are well identified in the IGN database). Overall, the IGN DB forest appears as the most accurate forest database and was thus primarily selected to be used in our PRA detection method. Sect. 4.2.4. assesses the sensitivity to this choice.

https://doi.org/10.5194/nhess-2022-177
Preprint. Discussion started: 19 July 2022
© Author(s) 2022. CC BY 4.0 License.

Natural Hazards and Earth System Sciences
Discussions
Open Access
EGU

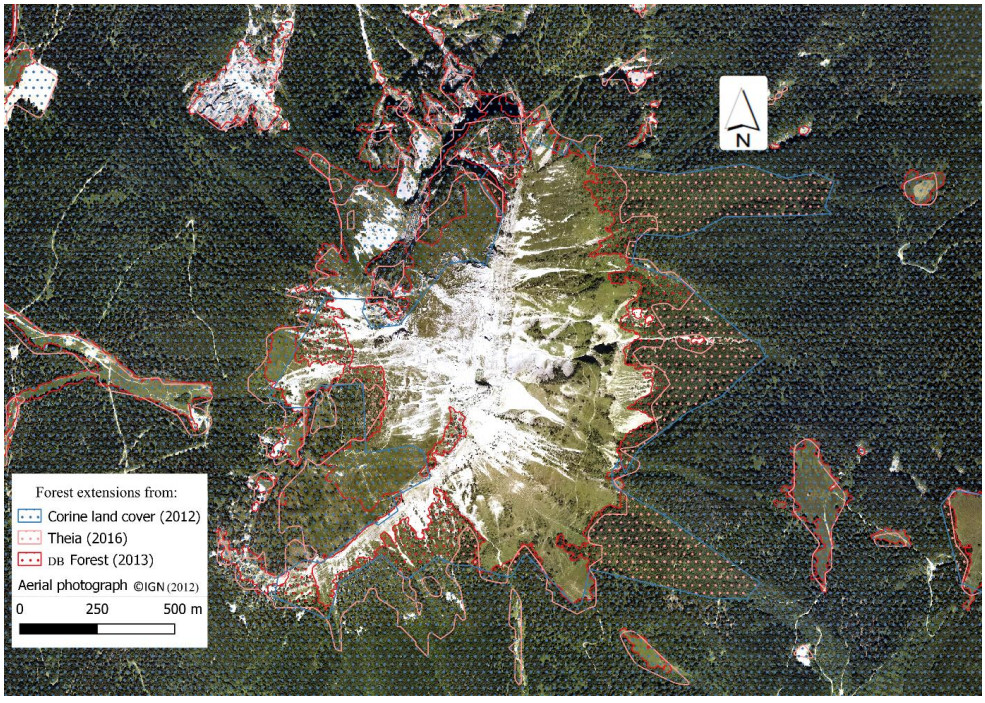

Figure 2: Comparison of forest extensions from Theia, Corine land cover, and DB Forest from IGN with aerial photographs (©IGN) taken in 2012 within the municipality of Le Sappey-en-Chartreuse, Chartreuse massif.

2.3 Avalanche extensions from the French avalanche cadastre (CLPA)

The lack of data concerning historical avalanches contributed to the Val-d'Isère disaster (11 February 1970), where an avalanche led to 39 casualties. Following this tragic event, the French government required the establishment of the CLPA cadastre. It consists in a collection of maps indicating the maximum extensions reached by avalanches in the past. CLPA is obtained using photo-interpretation, terrain observation, historical records, testimonies of residents and mountain professionals such as mountain guides, rescue services and ski resort professionals (Bourova et al., 2016; Naaim-Bouvet and Richard, 2015). CLPA also identifies protection structures and is mainly produced at the destination of mountain professionals (Ancey, 1996). CLPA now covers most of the French Alps, but some areas within the 23 massifs are still completely uncovered (Figure 3). CLPAs are updated regularly, and the whole information is freely available at http://www.avalanches.fr (Bonnefoy et al., 2010).

The overall objective of the CLPA is to map the entire avalanche terrain, independently of any frequency consideration. Arguably, with half a century of existence, CLPA extensions are getting closer and closer to the true maximal extension of avalanche terrain. From that perspective, the CLPA cadastre exactly corresponds to what we want to map with our PRAs, except that the CLPA does not distinguish release areas from flow paths and runout zones. Regarding the testimonies, iconographic sources and photo-interpretations on which it grounds, CLPA is very reliable, meaning that an avalanche extent which is within the CLPA is almost surely a true avalanche extent. By contrast, as all avalanche cadastres, CLPA is not entirely exhaustive. Very rare avalanches may not have occurred since the CLPA exists, and avalanches may have been missed in remote areas. In addition, forest stands that keep the footprints of past events in their landscape forms (e.g., Giacona et al., 2018) are absent

https://doi.org/10.5194/nhess-2022-177
Preprint. Discussion started: 19 July 2022
© Author(s) 2022. CC BY 4.0 License.

in high elevation areas. As a consequence, CLPA extensions are more exhaustive near human stakes like cities, villages and ski resorts, and less exhaustive in remote areas without stakes and which are difficult to access as well as in high elevation forest-free zones. This is for example the case for high mountain areas and/or remote valleys. Within the same line, CLPA extensions are often less exhaustive close to release areas than in runout areas. All in all, despite some limitations that may arguably be shared by many avalanche cadastres, the CLPA is a very valuable source of information regarding locations where past avalanches occurred, and, arguably, among the rare existing ones at a spatial scale as large as the entire French Alps (Bourova et al., 2016).

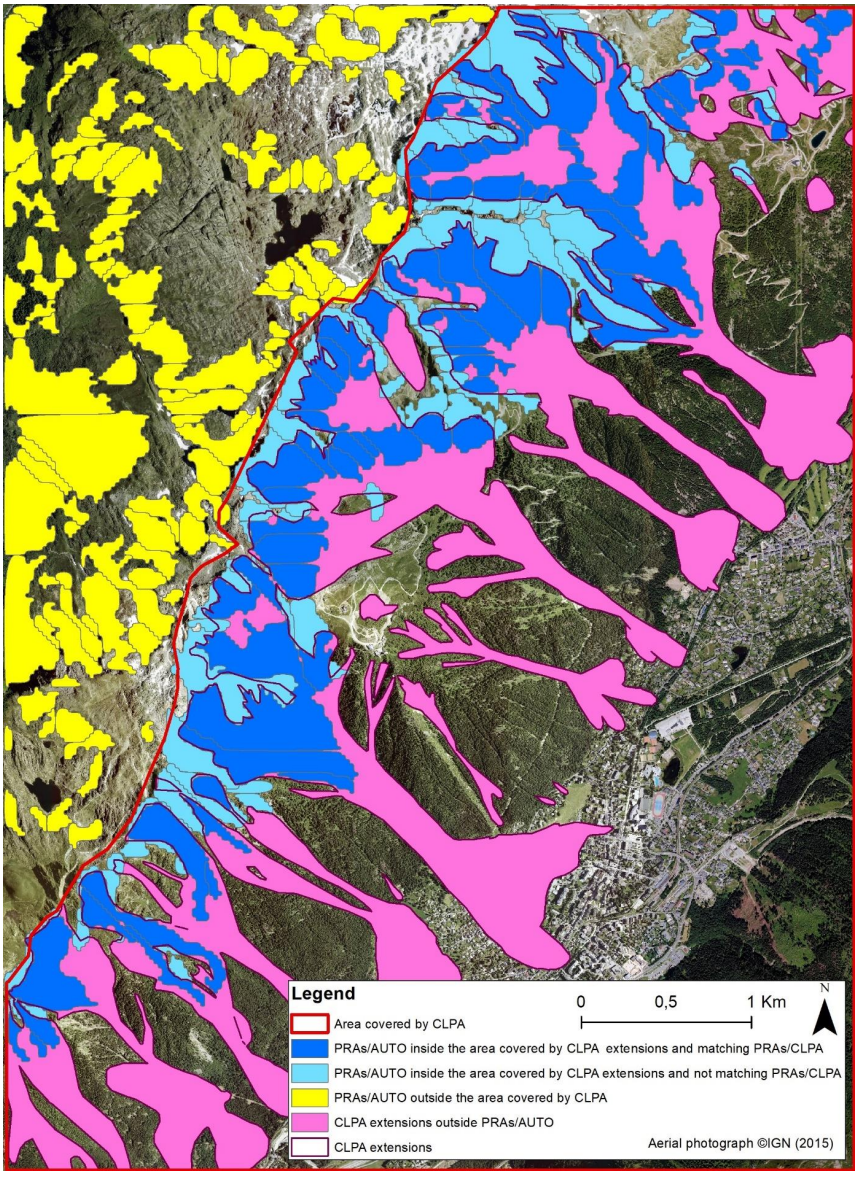

Figure 3: Result of the proposed PRA detection method (Figure 5) for the test area close to the town of Chamonix. Concordances and mismatches with the French avalanche cadastre (CLPA) are highlighted.

https://doi.org/10.5194/nhess-2022-177
Preprint. Discussion started: 19 July 2022
© Author(s) 2022. CC BY 4.0 License.

3. Proposed PRA detection method

3.1. Calculations at the pixel scale

In this study, the detection of individual PRAs uses topographical information (distance to ridges, slopes, aspect and general curvature) calculated at the pixel scale from the DEM and a watershed delineation algorithm. PRAs are detected without any consideration of release frequency, and identified PRAs correspond, for each avalanche path, to a maximal release extension.

3.1.1 Determination of ridges

To compute the distance to ridges, we use the Geomorphon algorithm of the Grass GIS described in Jasiewicz and Stepinski (2013), which processes the DEM to classify landform elements (ridge, valley) depending on topography. Once ridges have been obtained, the smallest distance to ridges can be evaluated for each pixel of the DEM (it can be equal to 0 when a PRA is in contact with a ridge).

3.1.2 Slope, aspect and curvature

Slope is directly obtained as the first derivate of the DEM, and curvature as the second derivate (i.e. first derivate of the slope). Aspect is the maximum slope direction. Concerning curvature, three different quantities can be considered:

- Profile curvature is the curvature of the surface towards the steeper slope;
- Plan curvature is the curvature of the surface transverse to the slope direction;
- General curvature is the curvature of the surface itself. General curvature is positive in convex areas such as ridges, negative in concave areas such as valleys, and null if the plan is horizontal (Zevenbergen and Thorne, 1987). We focus on this last quantity considered as the most relevant for snow avalanching.

Slopes, aspects and general curvatures are obtained using the default option in SAGA GIS (Zevenbergen and Thorne, 1987).

3.1.3 Individualization of PRAs using watersheds

In order to obtain spatial entities which correspond to individual avalanche paths/events, a delineation method is applied as follows (Figure 4). First, slopes are calculated for a central pixel and its eight neighbours. We then compute the flow direction (Stojkovic et al., 2012). Downward or negative slopes indicate the direction where water flows and provide the flow direction and flow accumulation. The number of accumulated pixels is then obtained for each pixel of the DEM as the sum of all pixels upstream, i.e. which converge in this direction. Flow accumulation is always non-zero except for pixels located on extremities (where flow accumulation is equal to zero). Individualized watersheds are obtained from this flow accumulation values by identifying the most important flows and by attributing each pixel to one of these flows.

https://doi.org/10.5194/nhess-2022-177
Preprint. Discussion started: 19 July 2022
© Author(s) 2022. CC BY 4.0 License.

Natural Hazards and Earth System Sciences
Discussions

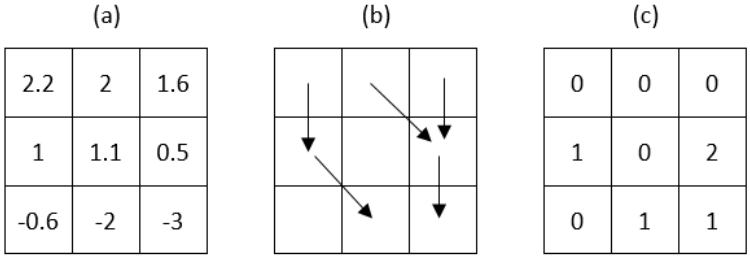

Figure 4: Principle of watershed delineation using flow direction: (a) Local slope for a central pixel and its eight neighbors (adapted from Kinner, 2003) (b) Calculation of flow direction (adapted from Stojkovic et al., 2012) (c) Result: flow accumulation.

3.2 The different steps of the proposed PRA detection method

Figure 5 presents the PRA detection method developed in this study, based on a DEM with a resolution of 25 m and forest cover extensions from IGN DB forest. Following most of existing approaches, it is a binary deterministic classification approach based on topographical parameters that do not change with time and on the presence/absence of forests. Thresholds and parameter values are chosen according to the literature, local peculiarities of the French Alps and a systematic parametric study (Sect. 4.2). Hence, with regards to existing methods, the main novelty is to include the watershed delineation step within the PRA identification. Our detection method is composed of three main steps, which can be further decomposed into 12 steps in total:

- The first main step consists in obtaining a layer of points corresponding to filtered pixels of the DEM and for which we evaluate slope, curvature, elevation, aspect, distance to the nearest ridge as stated above, as well as the name of the corresponding massif, latitude, and longitude. First, pixels below the altitude of 1400 m are excluded, as lower elevations receive few snow in the French Alps under current climate conditions (Durand et al., 2009b) and climate projections clearly indicate a further decrease of snow accumulations in the future for these low elevations (Castebrunet et al., 2014; Verfaillie et al., 2018). Second, following Maggioni and Gruber (2003), only pixels with a slope between 28° and 60° are kept. Third, only pixels situated at less than 600 m from the closest ridge are further considered. Figure S1 in the SM shows the pdf of the distance to the closest ridge for the study area close to Chamonix, which quickly decreases with distance and is close to zero above 600 m. Hence, even if this latter filter makes sense due to the impact of snowdrift on avalanche release, it affects limited areas. Eventually, the pixels kept are converted to a layer of points;
- The second step consists in removing areas covered by a dense forest according to the DB forest of IGN;
- The last step consists in applying the delineation algorithm to individualize each PRA (Sect. 3.1.3). Only polygons with a minimal area of ten pixels (e.g., 6249 m^2) are conserved. Indeed, very small PRAs are considered less prone to avalanches given the moderate amount of snow that can be accumulated on these surfaces. Also, an automated PRA detection method is primarily oriented towards large avalanches which are of interest to assess long-term risk for people and settlements downslope.

The resulting polygons are eventually converted to a vector layer. For each polygon corresponding to a PRA, different PRA-scale attributes are stored: distance to the closest ridge, name of the corresponding massif, slope, aspect, elevation, curvature, latitude, longitude, and area.

https://doi.org/10.5194/nhess-2022-177
Preprint. Discussion started: 19 July 2022
© Author(s) 2022. CC BY 4.0 License.

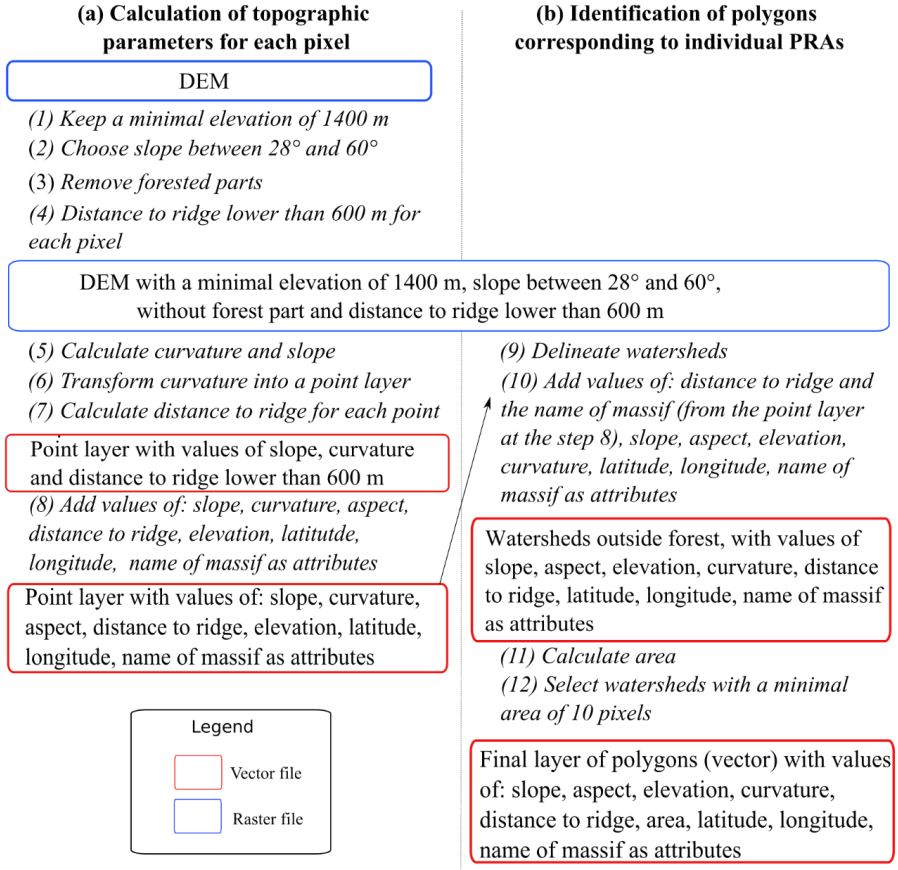

Figure 5: The 12 steps of the proposed PRA detection method. Calculations at (a) the pixel scale. (b) at the scale of identified polygons.

3.3 Processing of the CLPA for PRA evaluation

In this study, the evaluation of the accuracy of the detected PRAs is based on the CLPA cadaster. However, a direct comparison is meaningless. Indeed, i) there is simply no CLPA at all in some areas of the French Alps, ii) even in areas theoretically covered by CLPA, information about past avalanches in most remote zones can be missing, iii) path boundaries in CLPAs are not systematically mapped, especially in release areas. Furthermore, it is important to understand that the CLPA documents the entire maximum extensions of observed past avalanches, distinguishing photo-interpretations and testimonies, whereas our PRA detection approach only focuses on release areas. For these reasons, in order to evaluate our PRA detection method, CLPA extensions are processed as follows in order to isolate individual release areas within CLPA extensions that can be compared with our PRAs.

First, all boundaries of the CLPA polygons are merged together, leading a single polygon layer representing the maximal extent of past avalanches according to available records, testimonies and photo-interpretation insights. Second, the same criteria of slope, minimal elevation, distance to ridge, and presence of forest as for PRAS are used to filter this polygon. Eventually individual PRAs are identified with the watershed delineation algorithm,

https://doi.org/10.5194/nhess-2022-177
Preprint. Discussion started: 19 July 2022
© Author(s) 2022. CC BY 4.0 License.

Natural Hazards and Earth System Sciences
Discussions
Open Access
EGU

and those with a minimal area of 10 pixels are kept (Figure 6). This provides spatial entities fully comparable to automated PRAs. Sect. 5 further discusses pro's and con's of this processing approach to automated PRA detection evaluation.

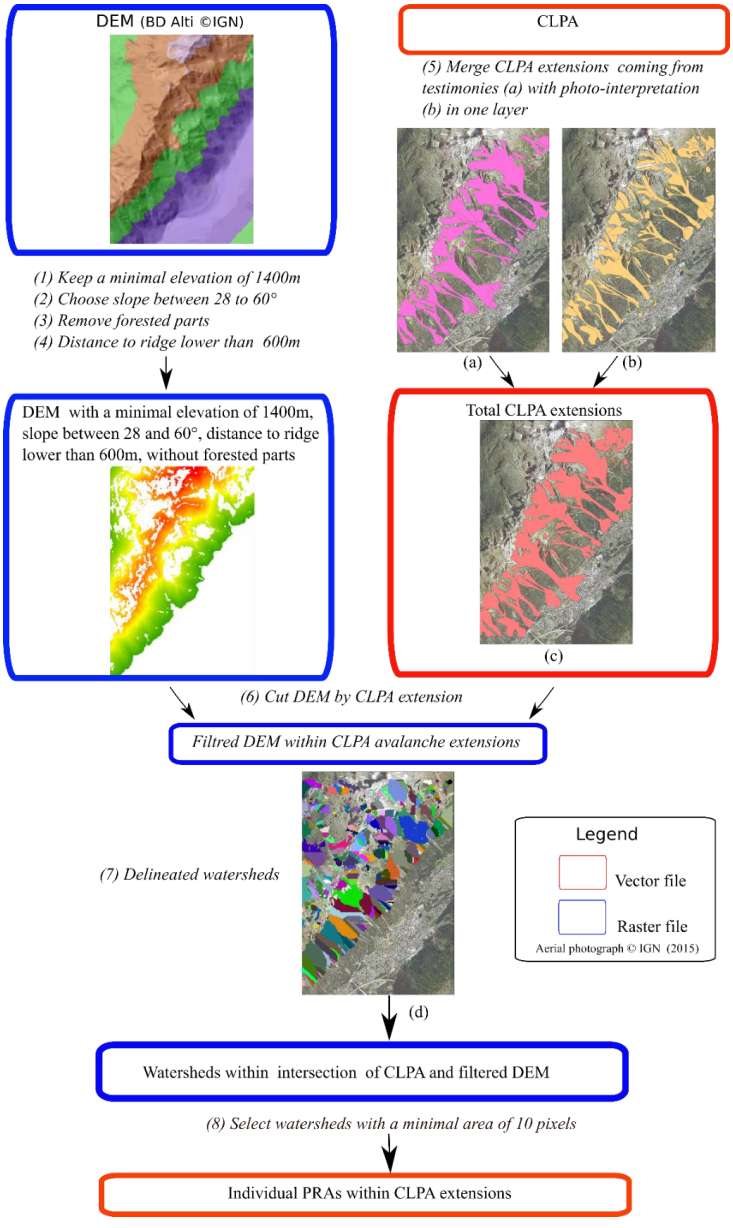

285

Figure 6: Processing of the French avalanche cadaster (CLPA) that identifies individual PRAs within CLPA avalanche extensions as a validation support for the proposed PRAs detection method. (a) CLPA avalanche extensions coming from testimonies. (b) CLPA avalanche extensions coming from photo-interpretation. (c) Union of CLPA avalanche extensions. (d) Delineation of individual watersheds within CLPA avalanche extensions. Aerial photograph ©IGN 2015.

https://doi.org/10.5194/nhess-2022-177
Preprint. Discussion started: 19 July 2022
© Author(s) 2022. CC BY 4.0 License.

Natural Hazards and Earth System Sciences
Discussions

3.4 Confusion matrices and evaluation scores

Confusion matrices (Table 1) can be obtained from the comparison between the detected PRAs and the processed CLPA extensions (Sect. 3.3), the latter being considered as a reference dataset (ground truth). A confusion matrix includes four numbers (or rates, i.e. standardized numbers): true positives (TP), true negatives (TN), false positives (FP), and false negatives (FN). A true positive means that the prediction and the reference values match, i.e. detected PRAs match processed CLPA extensions. A false positive means that a PRA is detected outside the processed CLPA extensions. By construction, the false positive rate is one hundred percent less the true positive rate. True negatives correspond to areas which are neither detected by our PRA detection method nor included in processed CLPA extensions, and false negatives to processed CLPA extensions that are not detected by our method. As the CLPA processing method applies the same filters than our PRA detection method and because the comparison is restricted to the area covered by CLPA extensions (Sect. 3.3), by construction, the true negative rate equals 100% and the false negative rate equals 0%.

		Detected PRAs	
		Yes	No
Processed CLPA extensions	Yes	True positive (TP)	False negative (FN)
	No	False positive (FP)	True negative (TN)

Table 1 : Principle of a confusion matrix and application to our PRA detection method.

Accuracy and error rates that sum up the confusion matrix are classically computed as follows:

$$Accuracy\ rate = \frac{True\ positive + True\ negative}{True\ positive + True\ negative + False\ positive + False\ negative}\ , \quad (1)$$

$$\text{Error rate} = \frac{False\ positive + False\ negative}{True\ positive + True\ negative + False\ positive + False\ negative}\ . \quad (2)$$

Since, in our case, the true negative rate equals 100%, these resume to:

$$Accuracy\ rate = \frac{(True\ positive + 100)}{200}\ , \quad (3)$$

$$\text{Error rate} = \left(\frac{\text{False positive}}{200}\right)\ . \quad (4)$$

Eventually, to evaluate the ability of our method to detect i) the right number of PRAs and ii) their correct extension, the confusion matrix is computed both in terms of areas (comparison of the areas of the polygons) and numbers (comparison of the number of polygons).

4 Results

4.1 Results for test areas and massifs

We first illustrate the results of the PRA detection method with the small area close to Chamonix (Figure 3). Avalanche extensions from the CLPA, when processed according to Sect. 3.3, lead to 85 individual PRAs in this area (PRAs/CLPA). For the same area, the automated detection method leads to 107 PRAs within the area covered by CLPA, and to 103 PRAs outside (PRAs/AUTO outside the area covered by CLPA). The latter illustrate remote areas not covered by CLPA, Chamonix city being surrounded by high mountains, which are difficult to access and document.

https://doi.org/10.5194/nhess-2022-177
Preprint. Discussion started: 19 July 2022
© Author(s) 2022. CC BY 4.0 License.

Among the 107 PRAs detected within the area covered by CLPA, 90 intersect the processed CLPA extensions (PRAs/AUTO inside the areas covered by CLPA and matching PRA/CLPAs). By contrast, 17 PRAs detected within the area covered by CLPA do not intersect the processed CLPA extensions at all (PRAs/AUTO inside the areas covered by CLPA and not matching PRA/CLPAs).

The two confusions matrices are computed for the areas covered by CLPA only. They evaluate the performances of the detection method in terms of number and surface of detected PRAS. In numbers, the 90 detected PRAs that intersect the processed CLPA extensions represent 84.1% of the total number of detected areas within the areas covered by CLPA (true positives, table 2). We remind that the "false positive" cases (15.9%) complements the "true positive" and that 100% of CLPA avalanches are detected according to our evaluation approach, by constraint. We obtain an accuracy rate in number of 92.1% and an error rate of 7.9% (Eqs. 8-9). In term of areas, the total area covered by the detected PRAs in the areas covered by CLPA is 5.48 km^2 (Table 2), and, among them, 5.29 km^2 intersect CLPA extensions (96.5 % of true positives). We obtain an accuracy rate of 98.3 %, and consequently an error rate of 1.7% in terms of areas.

Confusion matrix in areas [km^2] (%)		Confusion matrix in numbers (%)	
5.29 km^2 (96.5%)	0 (0%)	90 (84.1%)	0(0%)
0.19 km^2 (3.5%)	3.56 km^2 (100%)	17 (15.9%)	85 (100%)

Table 2 : Confusion matrix in areas (%) and numbers (%) for the test area close to Chamonix.

Figure 7 presents massif-scale results of the PRA detection method for the massif of Chartreuse. For this massif, the area covered by CLPA is located on the east flank of the massif along a main ridge and close to the large Gresivaudan valley, which is densely urbanized. Visually, the matching between the PRAs within processed CLPA extensions and the automatically detected PRAs, is excellent. Accuracy rates reach 93.5% in numbers and 96.2% in areas (still computed for the areas covered by CLPA only). Logically, detected PRAs are concentrated close to the ridge, where the only areas in the massif of Chartreuse that are both high and steep enough and forest free are located.

Table 3 sums up accuracy and error rates for the massifs of Chartreuse, Maurienne and Mont-Blanc, the results for the Chamonix test area being also reported for the sake of comparison. While the accuracy rates are similar to those obtained in the Chamonix test area for the massif of Chartreuse and Maurienne, they are slightly lower for the entire massif of Mont-Blanc, notably in numbers (89.8% versus 92.1-93.5% in the two other massifs). Yet, even in the Mont-Blanc massif, accuracy remains always high, especially in areas.

Figs. S2-S3 in the SM displays massif-scale results for the Mont-Blanc and Maurienne massifs. Both of them are largely covered by CLPA, making the obtained accuracy rates even more probative (i.e. they are computed over large areas / a large number of PRAs). The lower accuracy rates for the massif of Mont-Blanc can probably be explained by the fact that avalanche activity is, on average, more exhaustively documented close to release areas with the extension of CLPAs in the massifs of Chartreuse and Maurienne. The reason is that, in the Mont-Blanc massif, many avalanche release areas included within the area covered by CLPA (South-East of Figure S2 in SM) are located at high elevations and in remote zones, and very far from any forest stand. Hence, related avalanche activity was missed during the establishment of CLPAs, as no insights from past snow avalanches could be retrieved, either from testimonies or from photo-interpretation (visual detection of avalanche corridors in forested

https://doi.org/10.5194/nhess-2022-177
Preprint. Discussion started: 19 July 2022
© Author(s) 2022. CC BY 4.0 License.

Natural Hazards and Earth System Sciences
Discussions
Open Access
EGU

slopes). By comparison, in Maurienne and Chartreuse, PRAs in areas covered by CLPA are, on average, located closer to valleys and forest stands, making arguably CLPAs more accurate close to release areas in these massifs.

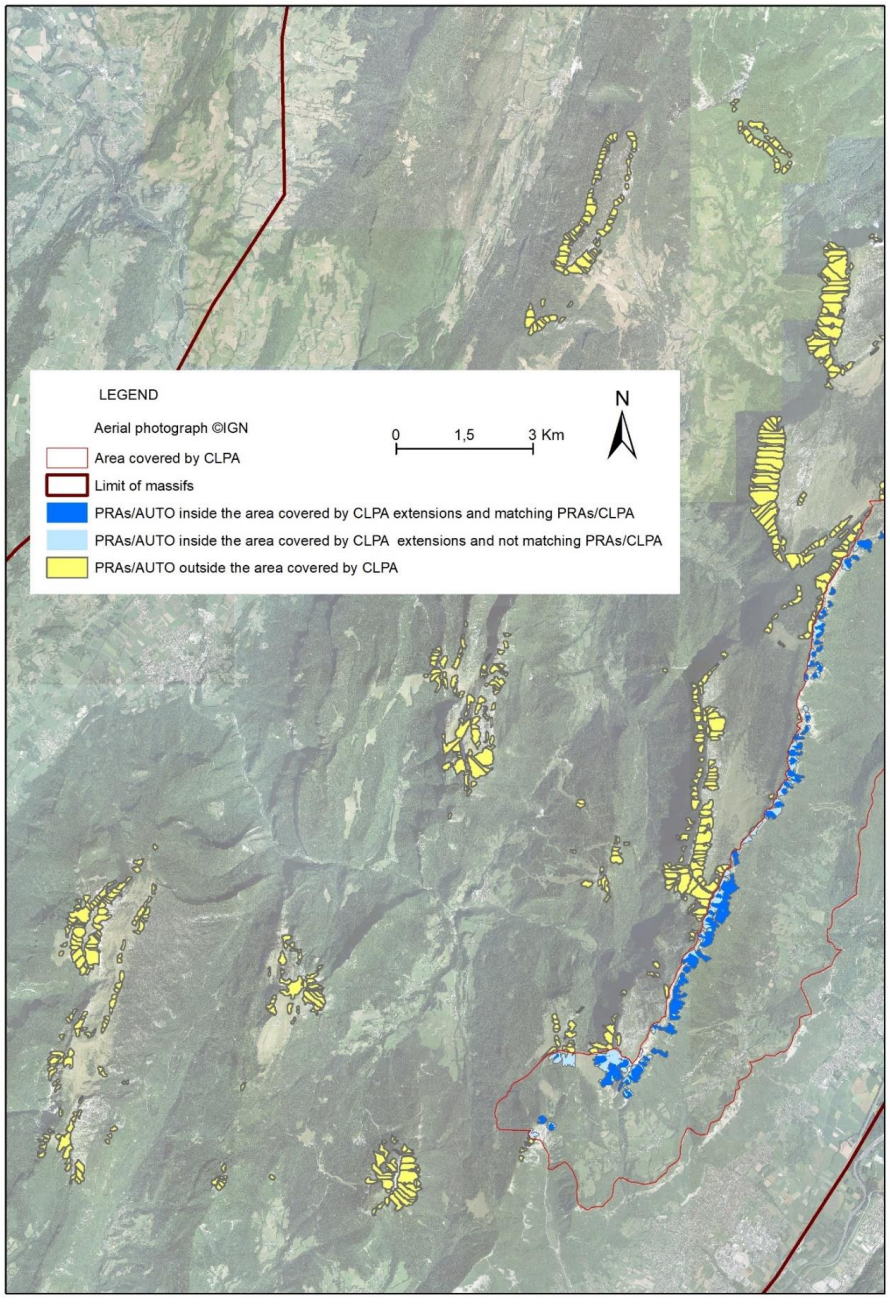

360 **Figure 7 : Result of the proposed PRA detection method (Figure 5) for the entire Chartreuse massif.**

https://doi.org/10.5194/nhess-2022-177
Preprint. Discussion started: 19 July 2022
© Author(s) 2022. CC BY 4.0 License.

		Chamonix test area	Chartreuse Massif	Maurienne Massif	Mont-Blanc Massif
In numbers	Accuracy rate (Eq. 3)	92.1	93.5	92.1	89.8
	Error rate (Eq. 4)	7.9	6.5	7.9	10.1
In areas	Accuracy rate (Eq. 3)	98.3	96.2	97.1	96.7
	Error rate (Eq. 4)	1.7	3.8	2.9	3.3

Table 3 : Summary of accuracy scores calculated in numbers (%) and areas (%) for the different test areas and massifs.

4.2 Sensitivity study

Factors involved in the PRA detection method are the minimal elevation, the range of relevant slopes, the maximum distance to ridges, the presence of forest, the minimum size of detected PRAs and the segmentation using watershed delineation. In order to provide insights about the respective weight of these factors, and more generally to assess the sensitivity of our PRA detection method, a parametric study is conducted focusing on the study area close to Chamonix. We first quantify to which extent the successive steps of the detection method gradually increase accuracy rates. In a second time, we more deeply analyse the sensitivity to the most critical factors.

4.2.1 Successive steps of the detection method

Table 4 presents the accuracy and error rates (in numbers and in areas) when the different filters of our detection method are applied successively. First, we see that an accuracy rate of 73.7% in numbers is obtained with the filter on elevation (1400 m a.s.l.) alone. The supplementary effect of the filter on the slope range is rather moderate (accuracy rate increases from 73.7% to 75.5%). The reason is that, for this test area, this filter is not very restrictive, as most of the terrain is very steep. Same holds for the effect of the maximum distance to ridges: a significant gain, but moderate as the filter is not very restrictive (Fig S1 in SM showing that the fraction of terrain located above 600 m from the closest ridge is very small). The filtering of forested areas improves the detection more largely (accuracy rate rises from 77.4% to 81%). Finally, the selection of PRAs with a minimal size of ten 25 m x 25 m pixels greatly improves the comparison of the number of PRAs obtained with our detection method and from the CLPA (accuracy rate rises from 81% to 92.1%). More or less the same conclusion holds if the analysis in conducted in terms of area. An exception in that, logically, the effect of the threshold on the minimal area has much less effect that for the analysis in terms of PRA numbers, as this filter removes only a few pixels, modifying the PRA extensions only very slightly. This all confirms in a pragmatic way the usefulness of all the different steps of the method, even if the effect of one specific filter can be relatively marginal (especially if accuracy scores are already high before applying the considered specific filter).

		Elevation	Slope	Distance to ridge	Forest	Minimal area
In numbers	Accuracy rate	73.7	75.5	77.4	81	92.1
	Error rate	26.3	24.5	22.6	19	7.9
In areas	Accuracy rate	97	94.6	94.7	98.3	98.3
	Error rate	3	5.4	5.3	1.7	1.7

Table 4 : Evolution of accuracy and error rates in numbers (%) and areas (%) when applying the different steps/filters of the method successively, test area close to Chamonix.

https://doi.org/10.5194/nhess-2022-177
Preprint. Discussion started: 19 July 2022
© Author(s) 2022. CC BY 4.0 License.

4.2.2 Effect of the minimal elevation threshold

Table 5 reports the performances with/without the minimal elevation filter. By contrast to the first column of Table 4, here the comparison is with all steps of the method with/without the specific elevation threshold filter. Without the latter, additional PRAs are detected at low elevations (from 1193 to 1400 m a.s.l.), notably in rather unrealistic locations (if avalanches were actually released at these locations, testimonies would definitely have been available and included in CLPAs). Hence, the filter logically increases accuracy rates, confirming its usefulness.

		With a minimal elevation of 1400 m a.s.l.	Without a minimal elevation of 1400 m a.s.l.
In numbers	Accuracy rate	92.1	70.5
	Error rate	7.9	29.5
In areas	Accuracy rate	98.3	93
	Error rate	1.7	7

Table 5 : Accuracy and error rates (%) with and without a minimal elevation of 1400 m a.s.l., test area close to Chamonix.

4.2.3 Effect of the slope range

To quantify the effect of the slope range, we compare PRAs obtained when applying different slope intervals 28-60°, 29-60°, and 30-60°. With larger intervals of slopes, more pixels are obviously included within PRAs. For example, the most restrictive range tested (slopes between 30° and 60°) leads to the identification of 218 PRAs in the test area, while the widest range (28-60°) leads to 227 PRAs without decreasing accuracy rates and with the identified PRAs remaining at realistic locations (Figure 8a). We therefore keep the latter larger range, even if considering any of the other tested alternatives would, in fine, not make a large difference.

4.2.4 Comparison of the performances with the different forest databases

Table 6 compares the accuracy and error rates obtained with the different nation-wide forest databases introduced in Sect. 2.2. When forest areas are not removed at all, we obtain the lowest accuracy rates in numbers and areas. This shows the interest of the forest filter to exclude correctly many areas where avalanche release are virtually impossible. By contrast, we obtain the highest accuracy rates when the DB forest from IGN is used (92.1% in numbers and 98.3 % in areas).

		Without forest	Theia	Corine land cover	DB forest
In numbers	Accuracy rate	81	77.6	82.1	92.1
	Error rate	19	22.4	17.9	7.9
In areas	Accuracy rate	98.3	89.4	92.7	98.3
	Error rate	1.7	10.6	7.3	1.7

Table 6 *:* Accuracy and error rates (%) as function of the forest data source: Theia, Corine land cover, DB forest, and without forest at all, test area close to Chamonix.

Figure 8b illustrates visually the differences in detected areas according to the forest database. With Theia, obtained PRAs cover 247 pixels in the test area close to Chamonix, which drops to 228 pixels with the Corine land

https://doi.org/10.5194/nhess-2022-177
Preprint. Discussion started: 19 July 2022
© Author(s) 2022. CC BY 4.0 License.

cover forest data and to 227 pixels with the forest data of DB forest from IGN. In details, some forested areas obtained from Corine land cover seem to correspond to grasslands according to the aerial photograph, mainly at forest boundaries. In addition, for some low elevation areas, Corine land cover and Theia both indicate dense forests that actually do not exist. Eventually, forested areas provided by Theia are, at some locations, too segmented with regards to reality, which makes that some small PRAs are unrealistically detected when this data is used in some small areas where forest is present in reality. On the contrary, using the DB forest data from IGN, detected PRAS mostly only correspond to high elevations that are forest-free according to the aerial photograph. Only one PRA remains detected at a low elevation near the pylon of a chairlift. This corresponds to an area where a large hiking trail eroded by walkers prevents the forest development, making an avalanche release actually possible, as slope is favorable. All in all, not only the DB forest is arguably the most representative of terrain reality (Figure 2), but its inclusion within the detection method provides the most numerically accurate and visually realistic results.

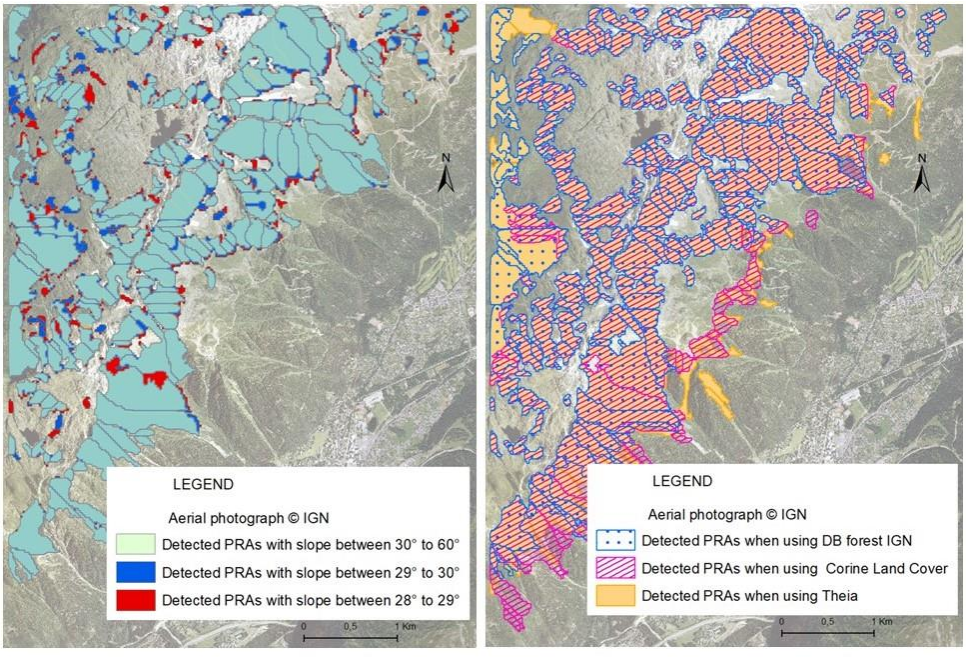

Figure 8 : (a) Effect of the range of slopes on detected areas, and (b) effect of forest data source on detected areas, test area close to Chamonix. Aerial photograph ©IGN 2015.

4.2.5 Impact of the delineation algorithm

Table 7 eventually compares the performances with/without the application of a delineation algorithm to identify individual PRAs. As expected, the individualization of the PRAs has mostly an impact on the number of PRAs, increasing the accuracy rate greatly, from 63.6% to 92.1%. This shows its crucial role to identify PRAs corresponding to realistic individual avalanche paths/events. By contrast, a slight decrease of the accuracy in areas (from 98.7% to 98.3%) is observed. The reason is that keeping PRAs of at least ten pixels only removes very small

https://doi.org/10.5194/nhess-2022-177
Preprint. Discussion started: 19 July 2022
© Author(s) 2022. CC BY 4.0 License.

areas when the watershed delineation is used that are kept when it is not. Hence inclusion of the watershed delineation algorithm excludes some small areas that were actually part of CLPA extensions. Yet, this effect is very small, and more than largely compensated by the large increase in accuracy regarding PRA numbers / individualisation.

		DEM with watersheds	DEM without watersheds
In numbers	Accuracy rate	92.1	63.6
	Error rate	6.7	36.4
In areas	Accuracy rate	98.3	98.7
	Error rate	1.5	1.3

Table 7 : Accuracy and error rates (%) with and without watershed delineation.

5 Discussion, conclusion and outlooks

5.1 Main outcomes of the work

Avalanche risk assessment is an important issue for the reduction of human causalities and property damages in mountain regions. While past avalanches provide data about dimension and types of avalanches that could occur in the future, this source of information is far from exhaustive and remains limited to specific monitored areas. Notably, information about avalanche release areas is sparse since the mountain terrain is huge and not always accessible. To map and mitigate avalanche risk at large scales, the automatic detection of PRAs is thus a powerful solution, notably to provide inputs for an avalanche simulation software (e.g., Gruber and Bartelt, 2007). However, existing methods (e.g. Maggioni et al., 2002) suffer from i) a lack of systematic validation on the basis of adapted metrics and past observations over large areas and ii) a limited ability to distinguish PRAs corresponding to individual avalanche paths. To this aim, this study proposes a procedure for the automated detection of PRAs that classically uses topographical parameters and presence of forests as key factors, but includes watershed delineation within the PRA identification, which provides spatial entities more comparable to avalanche paths. PRAs are detected without any consideration of release frequency, and identified PRAs correspond, for each avalanche path, to a maximal release extension. Also, with regards to previous attempts, a stronger emphasis is put on the evaluation of its performances using a set of different metrics (accuracy scores for PRA numbers and areas) by comparison to the CLPA, a long and systematic record of past avalanche extents. Eventually, a comprehensive parametric and sensitivity study is performed, to guide the development of the method and identify parameter values and succession of steps which appear as reasonable in our context.

We developed and applied this method in/for three entire massifs of the French Alps, Chartreuse, Maurienne, and Mont-Blanc, demonstrating its applicability to large areas at reasonable computational costs, (e.g., among the considered test areas, the Mont-Blanc massif is 578 km^2). The evaluation of the performances showed that, logically, high accuracy can more easily be demonstrated in areas where avalanche activity is more exhaustively documented (e.g. higher accuracy rates in Chartreuse with regards to Mont-Blanc, for example). However, obtained accuracy rates were probative in all three test-massifs, between 89.8% and 93.5% in numbers and 96.2 and 97.1% in areas. The chosen three massifs rather well represent the diversity of altitudinal and lithological contexts of the French Alps. Our results therefore suggest that the method could be systematically used for the entire French Alps, a large territory where no automated PRA detection has been systematically implemented so

https://doi.org/10.5194/nhess-2022-177
Preprint. Discussion started: 19 July 2022
© Author(s) 2022. CC BY 4.0 License.

far to our knowledge. This will allow in the future the detection of PRAs within the 23 massifs even in areas which are still not covered by CLPA.

5.2 Selected factors and thresholds and comparison to existing methods

We remind that the final parameter/criterion retained within our PRA detection method are as follows: a minimal elevation of 1400 m, slopes between 28° and 60°, a distance to the closest ridge limited to 600 m, exclusion of the forested areas, the individualization of detected areas using a watershed delineation algorithm, and a minimal area of ten 25 m x 25 m pixels for the resulting PRAs. Most of these choices (except the novelty introduced by the watershed delineation) are well supported by several past studies (e.g., Maggioni et al, 2002).

As indicated above, a minimal elevation of 1400 m for snow avalanche release seems appropriate in the French Alps considering the limited amounts of snow precipitation expected in the future below this elevation. Yet, this threshold is dependent to the local climate and should be adapted for other regions. Our other choices regarding slope and distance to ridge are i) in accordance with the state of the art of PRA detection methods (Maggioni and Gruber, 2003; Bühler et al., 2013), ii) compatible with broader knowledge regarding snow avalanche formation (Schweizer et al., 2004), iii) well supported by our parametric study.

Our watershed delineation step slightly decreases the accuracy rate in terms of PRA areas, but greatly improves it in terms of PRAs numbers. As PRA detection is mostly oriented toward avalanche simulations to evaluate hazard and risk downslope, and given our definition of a PRA and our goal for their automatic delineation, we see this large gain in PRA number accuracy as crucial, and much more important that the slight loss in PRA area accuracy. It avoids unrealistically wide PRAs that correspond to different avalanche paths/events, which may allow performing simulations corresponding to realistic individual avalanche events.

Our sensitivity study showed higher accuracy rates both in numbers and areas when forested terrain was excluded than when this filter was not considered (Table 6). As forest cover is known to be effective to prevent avalanche release, this result is logical, but seeing it confirmed by ground truth is a supportive argument in favor of our method. Eventually, we demonstrated that, for the French Alps context, using the DB forest from IGN was the best choice among the different nation-wide forest data existing, being both the most representative of the reality of forest cover extensions and providing the best accuracy scores in terms of PRA detection.

The sensitivity analysis performed quantifies, by confrontation to the processed CLPA extensions, the sensitivity to different parametrizations and pragmatically identifies possible optimal choices, based on the best accuracy scores among competing solutions. Notably, Table 4 shows that our combination of choices leads to most sensible results, both in terms of PRA numbers and areas, and in a variety of massifs representative of the French Alps. Let us stress that our approach is not a direct comparison to existing algorithms and even less a claim of universal superiority. For this we would need i) to run all existing algorithms which for now are not available to the community as open access codes, and ii) to test the different existing algorithms on different datasets with different characteristics (resolutions, forest cover, topography, climate, etc.), as, possibly, there is no universal “best algorithm” for PRA detection. This large effort goes beyond the scope of this work, but could be envisaged in the future (Sect. 5.4).

https://doi.org/10.5194/nhess-2022-177
Preprint. Discussion started: 19 July 2022
© Author(s) 2022. CC BY 4.0 License.

5.3 Evaluation method

In order to evaluate the proposed PRA detection method, we confronted individualized detected PRAs to the CLPA, after isolating individual release areas within CLPA extensions. However, the quantification of the performances is impacted by the characteristics of the CLPA, being more or less easy depending on the presence/absence and varying exhaustiveness of CLPA extensions (Sect. 2.3). Notably, for areas within the French massifs not covered by CLPA, no performance quantification is obviously possible. Also, it is normal that some PRAs can be detected outside CLPA extensions, as we observe. This is especially the case in remote areas with no trees, where the CLPA may be less exhaustive than closer to the valleys and/or within forests. From this perspective, the results obtained in the different massifs and related accuracy rates are meaningful. By contrast, an avalanche extent which is within the CLPA is almost surely a true avalanche extent. Hence, the CLPA cannot bias the PRA detection towards false locations.

The fact that we apply the same filters to the CLPA extension and to the whole terrain on which PRAs also plays a role. First, our determination of release areas from CLPA extensions adds some uncertainty, e.g., presumably, we do not map release areas exactly within CLPA extensions but may integrate in PRAs from CLPA small parts of flow paths. However, determining from an avalanche that occurred, even if witnessed in real time and even more when observed a-posteriori, what exactly was the release area may be not easy at all, so that virtually any data source may include such uncertainty. Second, “false negatives” are impossible. In other words, PRAs considered as ground truth within CLPA extensions are necessarily identified by our method. We are thus unable to evaluate situations where our filters are too constraining, which may miss areas where avalanches could nevertheless be triggered.

All in all, the validation data we use is certainly not perfect and our validation approach may potentially favour the comparison with our detected PRAs, which may slightly contribute to the high accuracy scores we obtain. However, we recall that validation data regarding true release areas are very seldom, especially over large regions and none of them is arguably exhaustive (in terms of all potential areas) and free of errors (exact maximal extensions). At least the release areas that we derive from CLPA extensions are well available over large regions and exactly correspond to what we are searching: maximal extensions of individual events without any frequency consideration.

Eventually, we adapted devoted tools, confusion matrices and performance criteria that were seldomly used so far to evaluate PRA detection methods (to our knowledge, only in Bühler et al, 2018). Also, validation areas used in the literature are generally small. Here we performed the evaluation of our detection method over large areas (three massifs with diverse characteristics) and both in terms of numbers and areas. This demonstrated i) that, overall, our method performs satisfactory in the French Alps context, ii) the added value /sensitivity of/to each of its steps. We therefore believe that our systematic approach and rigorous framework is already an important step forward towards more objective PRA detection, to be further used for comparing different detection methods and/or in other contexts with different validation data. Notably, implementing our approach to other data sets would help understand to which extent the high scores we obtain i) are influenced by the validation framework, ii) can be reproduced elsewhere, iii) how the most critical parameter need to be changed to fit various conditions (e.g. lower minimal elevation in colder climate).

https://doi.org/10.5194/nhess-2022-177
Preprint. Discussion started: 19 July 2022
© Author(s) 2022. CC BY 4.0 License.

5.4 Outlooks

In this study, the PRA detection method was applied to three among the 23 massifs of the French Alps only. Future works may expand the effort to the 23 massifs and provide a detailed statistical assessment of the detected PRAs. This will improve our understanding of PRAs characteristics within the whole French Alps, and possibly allow identifying groups of massifs with common properties in terms of PRAs. This information could also be used, combined with available extreme snowfall/snow depth estimates (Gaume et al., 2013; Le Roux et al., 2021), for a large-scale mapping of avalanche hazard and risk in the French Alps using simulation tools, as already done in other countries such as Switzerland (e.g. Bühler et al., 2018; 2022). The most direct use of our PRAs is to consider all of them and, for each of them, their entire area, as well as "maximal" snow depths and "minimal" friction parameters for avalanche simulation. This may lead to the delineation of the entire avalanche prone terrain. To go further and evaluate hazard and risk levels downslope, obviously additional assumptions/choices are required regarding the magnitude and frequency of potentially triggered avalanche events. This may include several scenarios and/or the entire probability distribution for i) the frequency of trigger in each PRA, ii) the fraction of each PRA which is released, iii) the snow depth, iv) friction parameters, etc. Ultimately, results could be confronted to existing hazard assessment based on interpolation of existing avalanche runout data (Lavigne et al., 2015).

A second potential outlook would be to apply the method as it is in other mountain territories. Notably, rather close to the French Alps, the Pyrenees (Oller et al., 2021) and medium-high mountain ranges such as the Vosges Mountains (Giacona et al., 2017), which are prone to regular to strenuous avalanche activity, could be targeted. Yet, this would probably imply further tuning of some parameters of the method such as minimal elevation and distance to ridge, to adapt these to local peculiarities.

More ambitious outlooks relate to deeper improvements of the PRA detection method: i) make it dynamic to assess PRAs conditional to snow and weather conditions (e.g., Chueca Cía et al., 2014), ii) switch from deterministic to probabilistic detection rules (e.g., Kumar et al., 2019) to, e.g., include in it the uncertainty about the best parameter values to be used, and/or iii) use CLPA extensions not only as an evaluation support but as a training sample to determine PRAs using (object-based) classification algorithms. The added value of these different extensions could be systematically assessed using our evaluation framework and the data on which this study grounds.

Eventually, we hope that our data, now freely available for the community, and evaluation framework will, associated to other data sets, foster further benchmarks/inter-comparisons between already existing or new PRA detection methods. This may help drawing firmer conclusions regarding the respective efficiency of the different proposals in different contexts, as a contribution to safer mountain territories.

6 Acknowledgements

CD holds a PhD grant from Grenoble-Alpes University. Support from the French National Research Agency through the Statistical modelling for the assessment and mitigation of mountain risks in a changing environment - SMARTEN program (ANR-20-Tremplin-ERC8-0001) is acknowledged. INRAE is member of Labex OSUG.

https://doi.org/10.5194/nhess-2022-177
Preprint. Discussion started: 19 July 2022
© Author(s) 2022. CC BY 4.0 License.

7 Author's contribution

NE and GE designed the research. CD performed the analyses and drafted the first version of the manuscript. CD and MD produced the illustrations. All authors discussed the results and edited the manuscript.

8 Data availability

The source data and results of this study are available as: Duvillier, Cecile, Eckert, Nicolas, Evin, Guillaume, & Deschâtres, Michael. (2022). Development and validation using ground truth of a method to identify potential release areas of snow avalanches based on watershed delineation - source data (Version_1) [Data set]. Zenodo. https://doi.org/10.5281/zenodo.6517730. This data can be used to reproduce all the results of the paper and for further benchmarking of snow avalanche potential release area detection methods.

9 Code availably

The proposed PRA detection method has been developed using the QGIS free software and environment. It combines existing algorithms from the free softwares QGIS, SAGA, GDAL and GRASS, and from ArcGIS (for watershed delineations). Scripts can be requested to CD.

References

ADEME, IGN.: Contribution de l'IGN à l'établissement des bilans carbone des forêts des territoires (PCAET), 122-4, 2019.

Ammann, W., Bebi, P.: WSL Institute for Snow and Avalanche Research SLF, Der Lawinenwinter 1999, Ereignisanalyse, SLF Davos, 588 p, 2000.

Ancey, C.: Guide Neige et avalanches Connaissances, pratiques, sécurité. Paris: Editions Quae,1996.

Ancey, C., Rapin, F., & Taillandier, J. M.: Stratégie de protection des établissements hospitaliers de Saint-Hilaire-du-Touvet contre le risque d'avalanches. irstea. 108 p. ⟨hal-02578607⟩, 1999.

Ancey, C., Rapin, F., Martin, E., Coleou, C., Naaim, M., & Brunot, G.: L'avalanche de Péclerey du 9 février 1999. La Houille Blanche, (5), 45-53, 2000.

Arnalds, P., Jonasson, K., Sigurdson, S. T.: Avalanche hazard zoning in Iceland based on individual risk. Annals of Glaciology. 38. pp 285-290, 2004.

Aydin, A., and Eker, R.: GIS-based snow avalanche hazard mapping: Bayburt-Aşağı Dere catchment case. Journal of Environmental Biology, 38(5 (Special Issue)), 937-943, 2017.

Baghdadi, N., Selle, A., and Biagiotti, I.: Le Pôle Thématique National des Surfaces Continentales Theia. In La télédétection et les données aériennes au service de l'eau, 2021.

Barbolini, M., Pagliardi, M., Ferro, F., & Corradeghini, P.: Avalanche hazard mapping over large undocumented areas. Natural hazards, 56(2), 451-464, 2011.

Bartelt, P., Bühler, Y., Buser, O., Christen, M., & Meier, L.: Modeling mass-dependent flow regime transitions to predict the stopping and depositional behavior of snow avalanches. Journal of Geophysical Research: Earth Surface, 117(F1), 2012.

Bebi, P., Kulakowski, D., & Rixen, C.: Snow avalanche disturbances in forest ecosystems—State of research and implications for management. Forest ecology and Management, 257(9), 1883-1892, 2009.

Bertrand, M., Liébault, F., & Piégay, H.: Debris-flow susceptibility of upland catchments. Natural Hazards, 67(2), 497-511, 2013.

https://doi.org/10.5194/nhess-2022-177
Preprint. Discussion started: 19 July 2022
© Author(s) 2022. CC BY 4.0 License.

Bonnefoy, M., Borrel, G., Richard, D., Bélanger, L., & Naaim, M.: La carte de localisation des phénomènes d'avalanche (CLPA): enjeux et perspectives. Sciences Eaux Territoires, (2), 6-14, 2010.

Bourova, E., Maldonado, E., Leroy, J. B., Alouani, R., Eckert, N., Bonnefoy-Demongeot, M., and Deschatres, M .: A new web-based system to improve the monitoring of snow avalanche hazard in France, 2016.

Braun, T., Frigo, B., Chiaia, B., Bartelt, P., Famiani, D., Wassermann, J.: Seismic signature of the deadly snow avalanche of January 18, 2017, at Rigopiano (Italy). Scientific reports, 10(1), 1-10, 2020.

Bühler, Y., Hafner, E. D., Zweifel, B., Zesiger, M., & Heisig, H.: Where are the avalanches? Rapid mapping of a large snow avalanche period with optical satellites. Cryosph. Discuss, 119, 2019.

Bühler, Y., Kumar, S., Veitinger, J., Christen, M., Stoffel, A., and Snehmani, S.: Automated identification of potential snow avalanche release areas based on digital elevation models. Natural Hazards and Earth System Sciences, 13(5), 1321-1335, 2013.

Bühler, Y., von Rickenbach, D., Stoffel, A., Margreth, S., Stoffel, L., and Christen, M.: Automated snow avalanche release area delineation–validation of existing algorithms and proposition of a new object-based approach for large-scale hazard indication mapping. Natural Hazards and Earth System Sciences, 18(12), 3235-3251, 2018.

Bühler, Y. Bebi, P., Christen, M., Margreth, S., Stoffel, L., Stoffel, A., Marty, C., Schmucki, G., Caviezel, A., Kühne, R., Wohlwend, S., and Bartelt, P.: Automated avalanche hazard indication mapping on a statewide scale, Nat. Hazards Earth Syst. Sci., 22, 1825-1843, 2022.

Caetano, M., V. Nunes and A. Nunes.: CORINE Land Cover 2006 for Continental Portugal, Technical Report, Instituto Geográfico Português, 2009.

Castebrunet, H., Eckert, N., Giraud, G., Durand, Y., and Morin, S.: Projected changes of snow conditions and avalanche activity in a warming climate: the French Alps over the 2020-2050 and 20702100 periods, 2014.

Chueca Cía, J., Andrés, A. J., & Montañés Magallón, A.: A proposal for avalanche susceptibility mapping in the Pyrenees using GIS: the Formigal-Peyreget area (Sheet 145-I; scale 1: 25.000). Journal of Maps, 10(2), 203-210, 2014.

Durand, Y., Giraud, G., Laternser, M., Etchevers, P., Mérindol, L., and Lesaffre, B.: Reanalysis of 47 years of climate in the French Alps (1958–2005): climatology and trends for snow cover. Journal of applied meteorology and climatology, 48(12), 2487-2512, 2009a.

Durand, Y., Giraud, G., Laternser, M., Etchevers, P., Mérindol, L., & Lesaffre, B.: Reanalysis of 47 years of climate in the French Alps (1958–2005): climatology and trends for snow cover. Journal of applied meteorology and climatology, 48(12), 2487-2512, 2009b.

Eckert, N., Keylock, C. J., Bertrand, D., Parent, E., Faug, T., Favier, P., Naaim, M.: Quantitative risk and optimal design approaches in the snow avalanche field: Review and extensions. Cold Regions Science and Technology, 79, 1-19, 2012.

Eckert, N., Naaim, M., & Parent, É.: Long-term avalanche hazard assessment with a Bayesian depth-averaged propagation model. Journal of Glaciology, 56(198), 563-586, 2010.

Eckert, N., Naaim, M., Giacona, F., Favier, P., Lavigne, A., Richard, D., ... & Parent, E.: Repenser les fondements du zonage règlementaire des risques en montagne «récurrents». La Houille Blanche, (2), 38-67, 2018.

Evans, S.: General Geomorphometry, derivatives of altitude and descriptive statistics in: Chorley, R.J., Ed., Spatial Analysis in Geomorphology, Methuen & Co. Ltd., London, 17-90, 1972.

https://doi.org/10.5194/nhess-2022-177
Preprint. Discussion started: 19 July 2022
© Author(s) 2022. CC BY 4.0 License.

Evin, G., Sielenou, P. D., Eckert, N., Naveau, P., Hagenmuller, P., & Morin, S.: Extreme avalanche cycles: Return levels and probability distributions depending on snow and meteorological conditions. Weather and Climate Extremes, *33*, 100344, 2021.

Fischer, J. T., Kofler, A., Fellin, W., Granig, M., and Kleemayr, K.: Multivariate parameter optimization for computational snow avalanche simulation. Journal of Glaciology, 61(229), 875-888, 2015.

Gaume, J., Eckert, N., Chambon, G., Naaim, M., & Bel, L.: Mapping extreme snowfalls in the French Alps using max-stable processes. Water Resources Research, 49(2), 1079-1098, 2013.

Giacona, F., Eckert, N., & Martin, B.: A 240-year history of avalanche risk in the Vosges Mountains based on non-conventional (re) sources. Natural Hazards and Earth System Sciences, 17(6), 887-904, 2017.

Giacona, F., Eckert, N., Mainieri, R., Martin, B., Corona, C., Lopez-Saez, J., ... & Stoffel, M: Avalanche activity and socio-environmental changes leave strong footprints in forested landscapes: a case study in the Vosges medium-high mountain range. Annals of Glaciology, 59(77), 111-133, 2018.

Gruber, U., & Bartelt, P.: Snow avalanche hazard modelling of large areas using shallow water numerical methods and GIS. Environmental Modelling & Software, 22(10), 1472-1481, 2007.

IRASMOS Consortium.: Best practice of integral risk management of snow avalanches, rock avalanches and debris flows in Europe. Delivrable 5.4. Sixth Framework Programme (2002-2006). 138 p. available at: http://irasmos.slf.ch/results_wp5.htm, 2009.

Jasiewicz, J., and Stepinski, T. F.: Geomorphons a pattern recognition approach to classification and mapping of landforms. Geomorphology, 182, pp.147-156, 2013.

Karas, A., Karbou, F., Giffard-Roisin, S., Durand, P., & Eckert, N.: Automatic color detection-based method applied to sentinel-1 sar images for snow avalanche debris monitoring. IEEE Transactions on Geoscience and Remote Sensing, 2021.

Keylock, C. J., McClung, D. M., & Magnússon, M. M.: Avalanche risk mapping by simulation.: Journal of Glaciology, 45(150), 303-314, 1999.

Kinner, D. A.: Delineation and characterization of the Boulder Creek. Comprehensive Water Quality of the Boulder Creek Watershed, Colorado, During High-flow and Low-flow Conditions, 2000, 3(4054), 27, 2003.

Kumar, S., Srivastava, P. K., and Bhatiya, S.: Geospatial probabilistic modelling for release area mapping of snow avalanches. Cold Regions Science and Technology, 165, 102813, 2019.

Lavigne, A., Bel, L., Parent, E., & Eckert, N.: A model for spatio-temporal clustering using multinomial probit regression: application to avalanche counts. Environmetrics, 23(6), 522-534, 2012.

Lavigne, A., Eckert, N., Bel, L., & Parent, E.: Adding expert contributions to the spatiotemporal modelling of avalanche activity under different climatic influences. Journal of the Royal Statistical Society: Series C (Applied Statistics), 64(4), 651-671, 2015.

Lavigne, A., Eckert, N., Bel, L., Deschâtres, M., & Parent, E.: Modelling the spatio-temporal repartition of right-truncated data: an application to avalanche runout altitudes in Hautes-Savoie. Stochastic Environmental Research and Risk Assessment, 31(3), 629-644, 2017.

Le Roux, E., Evin, G., Eckert, N., Blanchet, J., & Morin, S.: Elevation-dependent trends in extreme snowfall in the French Alps from 1959 to 2019. The Cryosphere, 15(9), 4335-4356, 2021.

Lehning, M., Doorschot, J., & Bartelt, P.: A snowdrift index based on SNOWPACK model calculations. Annals of Glaciology, 31, 382-386, 2000.

https://doi.org/10.5194/nhess-2022-177
Preprint. Discussion started: 19 July 2022
© Author(s) 2022. CC BY 4.0 License.

Maggioni, M., and Gruber, U.: The influence of topographic parameters on avalanche release dimension and frequency. Cold Regions Science and Technology, 37(3), pp.407-419, 2003.

Maggioni, M., Gruber, U., and Stoffel, A.: Definition and characterisation of potential avalanche release areas. In Proceedings of the ESRI Conference, San Diego, 2002.

Naaim, M., Naaim-Bouvet, F., Faug, T., & Bouchet, A.: Dense snow avalanche modeling: flow, erosion, deposition and obstacle effects. Cold regions science and technology, 39(2-3), 193-204, 2004.

Naaim, M., Durand, Y., Eckert, N., & Chambon, G.: Dense avalanche friction coefficients: influence of physical properties of snow. Journal of Glaciology, 59(216), 771-782, 2013.

Naaim-Bouvet, F., and Richard, D.: Les risques naturels en montagne. Editions Quae, 2015.

Nolting, S., Marin, C., Steger, S., Schneiderbauer, S., Notarnicola, C., & Zebisch, M.: Regional scale statistical mapping of snow avalanche likelihood and its combination with an optical remote sensing based avalanche detection approach–first attempts for the province of South Tyrol (Italy), International snow science workshop 2018 (ISSW), Innsbruck, 2018.

Oller, P., Baeza, C., & Furdada, G.: Empirical α–β runout modelling of snow avalanches in the Catalan Pyrenees. Journal of Glaciology, 67(266), 1043-1054, 2021.

Ortner, G., Bründl, M., Kropf, C. M., Röösli, T., Bühler, Y., & Bresch, D. N.: Large-scale risk assessment on snow avalanche hazard in alpine regions. Natural Hazards and Earth System Sciences Discussions, 1-31, 2022.

Schweizer, J., Bruce Jamieson, J., & Schneebeli, M.: Snow avalanche formation. Reviews of Geophysics, 41(4), 2003.

Sielenou, P. D., Viallon-Galinier, L., Hagenmuller, P., Naveau, P., Morin, S., Dumont, M., ... & Eckert, N.: Combining random forests and class-balancing to discriminate between three classes of avalanche activity in the French Alps. Cold Regions Science and Technology, 187, 103276, 2021.

Stojkovic, M., Milivojevic, N., and Stojanovic, Z.: Use of information technology in hydrological analysis. E-society Journal, 105, 2012.

Sykes, J., Haegeli, P., & Bühler, Y.: Automated snow avalanche release area delineation in data sparse, remote, and forested regions. Natural Hazards and Earth System Sciences Discussions, 1-39, 2021.

Veitinger, J., Purves, R. S., and Sovilla, B.: Potential slab avalanche release area identification from estimated winter terrain: a multi-scale, fuzzy logic approach. Natural Hazards and Earth System Sciences, 16(10), 2211, 2016.

Verfaillie, D., Lafaysse, M., Déqué, M., Eckert, N., Lejeune, Y., and Morin, S.: Multi-component ensembles of future meteorological and natural snow conditions for 1500 m altitude in the Chartreuse mountain range, Northern French Alps. The Cryosphere, 12(4), 1249-1271, 2018.

Yariyan, P., Avand, M., Abbaspour, R. A., Karami, M., and Tiefenbacher, J. P.: GIS-based spatial modeling of snow avalanches using four novel ensemble models. Science of the Total Environment, 745, 141008, 2020.

Zevenbergen, L. W., and Thorne, C. R.: Quantitative analysis of land surface topography. Earth surface processes and landforms, 12(1), pp.47-56, 1987.

Zgheib, T., Giacona, F., Granet-Abisset, A. M., Morin, S., Lavigne, A., & Eckert, N.: Spatio-temporal variability of avalanche risk in the French Alps. Regional Environmental Change, 22(1), 1-18, 2022.